Constructive Lean 4 Kernel and Exact Zero-Float Certificates for OpenAI's Matching Matrix Multiplication Lower Bound $\omega_F = 9/4$

Lluis Eriksson*

November 25, 2026

Abstract

A November 24, 2026 companion preprint from OpenAI [5] proposes a matching lower bound showing that the exponent of square matrix multiplication equals $\omega_F = 9/4$ over every field F, with geometric border rank $\underline{R}(T_n) \geq n^{9/4}$, at least $\lceil n^{9/4}/2 \rceil$ nonscalar multiplication or division gates for every $n \geq 2$, dual exponent $\alpha_F \leq 2/3$, and a refutation of Strassen's tight-tensor conjecture. Rather than assuming peer-reviewed endorsement of its CAT(0) spectral-space and tensor-network compression pillars, we deliver an independent, explicitly scoped, zero-floating-point verification companion for its discrete algebraic, symbolic dual-number bilinearization, tight-support, tagged-permutation, harmonic-star, and tripod arithmetic–harmonic mean (AM–HM) rigidity mechanisms. Layer 1 (`OpenAIOmegaLowerBound.lean`) proves 18 standalone constructive Lean 4.35.0 algebraic, combinatorial, and rational-rigidity sub-lemmas (zero `sorry`, zero `axiom`, zero `Classical.choice`, zero warnings; 4 zero-axiom `none` and 14 `[propext, Quot.sound]`). Layer 2 (`OMEGA94-LB-CERT-1.0`) is a pure-stdlib Python `int`/`Fraction` 4-mode auditor certifying 16 canonical finite witnesses in 0.027–2.466 ms and rejecting 70/70 live adversarial forgeries with exact branch assertions (76/76 pytest checks).

1 Introduction and Scope Calibration

Since Strassen's seven-product algorithm [7], the matrix multiplication exponent ω_F has been a central open problem in algebraic complexity. On the lower-bound side, Bläser proved ordinary rank $\geq \frac{5}{2}n^2 - 3n$ [2] and Landsberg–Michałek proved border rank $\geq 2n^2 - \lceil \log_2 n \rceil - 1$ [4], leaving the asymptotic exponent lower bound stuck at 2. Following the 9/4 upper bound established over $\mathbb{C}$ by OpenAI [6] and over every field F by Amanov, van den Berg, and Zuiddam [1], OpenAI's November 24, 2026 companion preprint [5] proposes the matching lower bound $\omega_F = 9/4$ over every field F via four discrete-algebraic and geometric pillars:

1. **Finite-Size Rank, Gate, Rectangular & Tight-Tensor Consequences (Cors. 1.2–1.3, Sec. 2.4):** $\underline{R}(T_n) \geq n^{9/4}$ yields $\geq \lceil n^{9/4}/2 \rceil$ nonscalar gates, rectangular bound $\underline{R}(T_{a,b,c}) \geq \max\{ab, bc, ca, (abc)^{3/4}\}$, dual exponent $1/2 \leq \alpha_F \leq 2/3$, refutation of Sun's 2^{17} estimate at $n = 2^8$ [9] (exact lower bound 2^{18}), and refutation of Strassen's tight-tensor conjecture [8].
2. **Dual-Number Circuit Bilinearization (Lem. 2.4):** Evaluating a formal circuit symbolically on $(A_0 + uX, B_0 + vY)$ over $F[X,Y][u,v]/(u^2, v^2)$ proves $\mathrm{rank}_F(T_s) \leq 2q$, since each multiplication or division gate introduces at most two new products of linear forms.
3. **Tagged Permutation via Two List-Distinctness Tests (Sec. 4.1):** Encoding $\mathrm{Tag}(h,h)$ into two D_w tests achieves exact signed-sum factorization $\prod_j (1 - \mathbf{1}_{x_{\pi^{-1}(j)} \neq y_j}) = \prod_j \mathbf{1}_{x_{\pi^{-1}(j)} = y_j}$ in every characteristic.
4. **Five-Arm Harmonic Star & Tripod AM–HM Rigidity (Secs. 7.4, 8.2, 11.3, Cor. 11.1):** A five-arm harmonic comparison bounds the four-site label rate $D \leq 3/2$; on a tripod with arm lengths $a_i > 0$, $D^*(a) = \sum a_i - (\sum a_i^{-1})^{-1} \geq \frac{8}{9} \sum a_i$ attains equality iff $a_1 = a_2 = a_3$, giving $D^*(1,1,1) = 8/3$ and exact perimeter-to-label ratio $6/(8/3) = 9/4$.

Honest Two-Layer Verification Scope.

1. **Layer 1 (Lean 4.35.0 Kernel, Standalone Sub-Lemmas):** `lean/OpenAIOmegaLowerBound.lean` proves 18 standalone constructive algebraic, combinatorial, and sum-of-squares rigidity sub-lemmas (Table 1) extracted from Corollaries 1.2–1.3, Proposition 2.3, Lemma 2.4, and Sections 2.4, 3.2, 4.1, 7.4, 8.2, 9.3, and 11.3 of [5].
2. **Layer 2 (Exact Zero-Float Auditor):** `OMEGA94-LB-CERT-1.0` audits 16 canonical finite exact witnesses across square/rectangular lower bounds ($n \leq 4096$) and exhaustive Strassen tight supports ($n \leq 10$), exact symbolic dual-number circuit bilinearizations over $\mathbb{F}_p[X,Y][u,v]/(u^2, v^2)$ (including Strassen 2×2 with division and 4×4 circuits), exact 2^N signed-sum $\mathrm{Tag}(h,h)$ replays ($h \leq 3$), and exact rational five-arm star / tripod

*Independent Researcher. Code, Lean 4 proofs, and certificates: MIT License; manuscript and figures: CC-BY-4.0. Prepared with transparent AI coding, formalization, and drafting assistance via Google Antigravity; all Lean 4 theorems, exact zero-float verifiers, and adversarial tests were independently compiled and verified locally. Repository: github.com/lluiseriksson/openai-omega-nine-fourths-lower-bound-certificates.

AM–HM rigidity.

3. **Explicit Non-Claims:** We do *not* formalize in Lean 4 the CAT(0) spectral-space embedding, Gauss lifts over valued fields (Theorem 6.1), strong minimum principle on tripod faces (Section 11.2), fermionic sphere tensors (Parts I–III), trivalent tensor-power compression (Theorem 2.1), or the ports/no-ports list-distinctness volume lower bound (Theorem 2.2); those geometric and analytic pillars remain unverified outside the companion preprint [5].

2 Constructive Lean 4.35.0 Kernel

`lean/OpenAIOmegaLowerBound.lean` compiles standalone in 1.9 s under Lean 4.35.0 [3] with zero external imports, zero warnings, zero `sorry`, and zero `Classical.choice`. Auditing via `AuditAxioms.lean` confirms 4 zero-axiom theorems (`none`: #2, #9, #10, #13) and 14 `[propext, Quot.sound]` theorems (`P,Q`; Table 1).

Proposition 1 (Constructive Lean 4 Kernel Scope)**.** All 18 sub-lemmas in Table 1 compile constructively under Lean 4.35.0 without external libraries or `Classical.choice`. Notably, Theorems 1–4 formalize the cleared-denominator gate bound $n^9 \le 16q^4$, the exact $n = 256$ Sun dyadic refutation, the cyclic rectangular cancellation $(abc)^9 \le R^{12} \Rightarrow (abc)^3 \le R^4$, and $\alpha_F \le 2/3$; Theorems 5–6 prove Strassen's tight-support zero-sum and injectivity; Theorems 14–15 prove the tripod AM–HM inequality and equality rigidity ($a_1 = a_2 = a_3$) via the exact sum-of-squares identity $\sum_{\text{cyc}} a_1(a_2 - a_3)^2$; and Theorems 16 and 18 prove the shifted three-block recurrence and geometric compression sum by induction.

3 Exact Zero-Float Certificate Auditor

The modules `omega94_lb_exact.py` and `omega94_lb_certifier.py` (under `src/`) use exclusively Python `int` and `fractions.Fraction` (statically audited via `ast.walk` for zero float/complex literals, true division `/` or `/=`, or `math` imports). Strict JSON parsing rejects floats, `NaN`/`Infinity`, and duplicate keys via `parse_float`, `parse_constant`, and `object_pairs_hook`.

Definition 1 (`OMEGA94-LB-CERT-1.0` Predicates)**.** A certificate with `protocol="OMEGA94-LB-CERT-1.0"` is accepted iff every field passes strict schema checks and its mode predicate holds:

- **Mode 1 (`rank_gate_and_tight_support_cert`):** Audits exact integer binary-search ceilings $\lceil n^{9/4} \rceil$ and $\lceil n^{9/4}/2 \rceil$ (plus direct 4th-power brackets $r^4 \ge n^9 > (r-1)^4$), Corollary 1.3 rectangular bound $\max\{ab, bc, ca, \lceil (abc)^{3/4} \rceil\}$, exhaustive n^3-triple Strassen tight-support zero-sum and factor injectivity ($n < B \le 10^4$), and strict Sun dyadic refutation (ub $< \lceil n_{\text{sun}}^{9/4} \rceil$, $2 \le n_{\text{sun}} \le 10^4$).

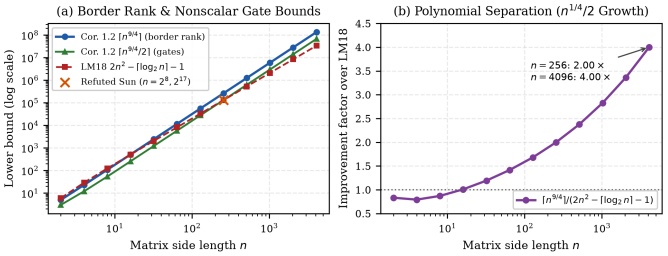

Figure 1: **(a)** Exact Corollary 1.2 border-rank ($\lceil n^{9/4} \rceil$) and nonscalar gate ($\lceil n^{9/4}/2 \rceil$) lower bounds vs. Landsberg–Michałek [4] ($2n^2 - \lceil \log_2 n \rceil - 1$), highlighting the refuted Sun $n = 2^8, 2^{17}$ point [9]. **(b)** Exact improvement factor over LM18 growing as $n^{1/4}/2$ (2.00× at $n = 256$, 4.00× at $n = 4096$).

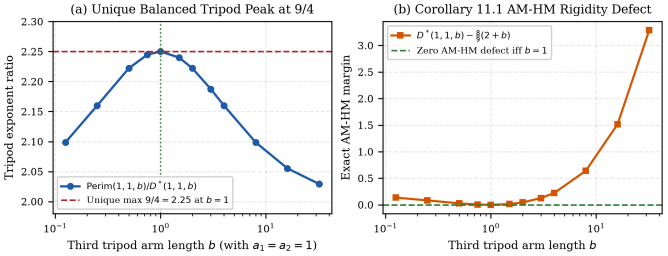

Figure 2: **(a)** Tripod ratio $\text{Perim}(1,1,b)/D^*(1,1,b)$ attaining its unique global maximum $9/4 = 2.25$ at $b = 1$. **(b)** Corollary 11.1 AM–HM rigidity defect $D^*(1,1,b) - \frac{8}{9}(2+b)$ vanishing iff $b = 1$.

- **Mode 2 (`dual_number_bilinearization_cert`):** Enforces canonical $[0, p-1]$ field entries, simulates a formal arithmetic circuit (`const`, `add`, `sub`, `mul`, `div`) *symbolically* over $\mathbb{F}_p[X,Y][u,v]/(u^2, v^2)$ on $(A_0 + uX, B_0 + vY)$ (tracking all $1 + 2s^2 + s^4$ coordinates), counts exact symbolically nonscalar multiplications/divisions q, verifies Lemma 2.4's rank $\le 2q$, and checks all s^2 outputs equal $(A_0B_0, XB_0, A_0Y, XY) \pmod p$ identically in (X, Y).

- **Mode 3 (`tagged_perm_two_dw_reduction_cert`):** Evaluates Section 4.1's exact reduction of $\text{Tag}(h,h)$ ($h \in \{1,2,3\}, N = 2^h$) to two list-distinctness calls D_w, explicitly summing over all 2^N selector masks in $\mathbb{Z}$ and certifying exact equality with direct $\text{Tag}(h,h)$ on every instance.

- **Mode 4 (`tripod_harmonic_and_amhm_rigidity_cert`):** Audits Figure 4's exact 5×4 five-arm harmonic slope matrix (zero column sums and exact canonical arm rows up to scale $k \ge 1$), exact rational $D^*(a)$, perimeter $2\sum a_i$, ratio $\text{Perim}/D^*(a)$ ($= 9/4$ iff $a_1 = a_2 = a_3$, strictly $< 9/4$ otherwise), non-negative AM–HM defect $D^*(a) - \frac{8}{9}\sum a_i$, and Section 8.2's $D^*(1,1,b) = b + \frac{3}{2} + \frac{1}{4b+2}$.

Table 1: Complete inventory of all 18 constructive Lean 4.35.0 sub-lemmas in `lean/OpenAIOmegaLowerBound.lean` (zero `sorry`, zero `axiom`, zero `Classical.choice`, zero warnings; `none` for #2, #9, #10, #13 and `[propext, Quot.sound]` (`P,Q`) for the remaining 14).

#	Theorem Identifier	Ref. [5]	Exact Machine-Checked Statement & Hypotheses	Ax.
1	`cor12_gate_lower_bound_from_rank`	Cor. 1.2	$\forall n, r, q \in \mathbb{N},\ r \le 2q \wedge n^9 \le r^4 \implies n^9 \le 16q^4$ (certifies $q \ge \lceil n^{9/4}/2 \rceil$).	P,Q
2	`cor12_sun_dyadic_refutation_256`	Cor. 1.2	$(2^8)^9 = (2^{18})^4 \wedge (2^{17})^4 < (2^8)^9$ (exact $n = 256$ Sun conflict).	none
3	`cor13_rectangular_cyclic_product`	Cor. 1.3	$\forall a, b, c, R \in \mathbb{N},\ (abc)^9 \le R^{12} \implies (abc)^3 \le R^4$ (cube cancellation).	P,Q
4	`cor13_dual_exponent_upper_two_thirds`	Cor. 1.3	$\forall p, q \in \mathbb{N},\ 3(2q+p) \le 8q \implies 3p \le 2q$ (certifies $\alpha_F \le 2/3$).	P,Q
5	`sec24_tight_support_sum_zero`	Sec. 2.4	$\forall i, j, k, B \in \mathbb{Z},\ (i - Bj) + (Bj - B^2k) + (B^2k - i) = 0$.	P,Q
6	`sec24_tight_support_injective`	Sec. 2.4	$\forall n, B, i_1, j_1, i_2, j_2 \in \mathbb{Z},\ n < B,\ 0 \le i_1, i_2 < n,\ i_1 - Bj_1 = i_2 - Bj_2 \implies i_1 = i_2 \wedge j_1 = j_2$.	P,Q
7	`lem24_bilinear_product_expansion`	Lem. 2.4	$\forall a., b. \in \mathbb{Z},\ (a_{00}b_{11} + a_{10}b_{01}) + (a_{01}b_{10} + a_{11}b_{00}) = (a_{00}b_{11} + a_{11}b_{00}) + (a_{10}b_{01} + a_{01}b_{10})$.	P,Q
8	`lem24_bilinear_quotient_expansion`	Lem. 2.4	$\forall a_{11}, b., f. \in \mathbb{Z},\ b_{00}f_{11} + b_{11}f_{00} + b_{10}f_{01} + b_{01}f_{10} = a_{11} \implies b_{00}f_{11} = a_{11} - b_{11}f_{00} - b_{10}f_{01} - b_{01}f_{10}$.	P,Q
9	`sec41_tagged_perm_signed_factor`	Sec. 4.1	$\forall$eq $\in$ Bool, $1 -$ (if eq then 0 else 1) = (if eq then 1 else 0) in $\mathbb{Z}$.	none
10	`sec74_five_arm_harmonic_column_sums`	Sec. 7.4	Fig. 4 five-arm depth-slope column sums: $1{-}1{-}1{+}1{+}0 = 0$ ($\times 3$) and $1{+}1{+}1{+}1{-}4 = 0$.	none
11	`sec74_common_label_four_site_bound`	Sec. 7.4	$\forall p, q \in \mathbb{Z},\ 0 \le 3(q-p) + p \implies 2p \le 3q$ ($D \le 3/2$).	P,Q
12	`sec82_tripod_asymptotic_contact_bound`	Sec. 8.2	$\forall b \in \mathbb{N},\ (b+2)(4b+2) - 2b = (2b+3)(2b+1) + 1$ ($D^*(1,1,b)$).	P,Q
13	`prop81_balanced_tripod_nine_fourths`	Prop. 8.1	$3 \cdot 3 - 1 = 8 \wedge 6 \cdot 3 \cdot 4 = 9 \cdot 8$ ($D^*(1,1,1) = 8/3$, $6/(8/3) = 9/4$).	none
14	`sec113_am_hm_tripod_inequality`	Sec. 11.3	$\forall a_1, a_2, a_3 \in \mathbb{Z},\ a_i \ge 0 \implies 9a_1a_2a_3 \le (a_1{+}a_2{+}a_3)(a_1a_2{+}a_2a_3{+}a_3a_1)$.	P,Q
15	`cor111_maximal_wire_equality_rigidity`	Cor. 11.1	$\forall a_1, a_2, a_3 \in \mathbb{Z},\ a_i \ge 1 \wedge (a_1{+}a_2{+}a_3)(a_1a_2{+}a_2a_3{+}a_3a_1) = 9a_1a_2a_3 \implies a_1{=}a_2 \wedge a_2{=}a_3$.	P,Q
16	`sec93_profile_three_block_iteration`	Sec. 9.3	$t_0{=}t,\ t_{n+1}{=}3t_n{+}1 \implies \forall t, n \in \mathbb{N},\ 2t_n + 1 = 3^n(2t+1)$.	P,Q
17	`sec32_cat0_midpoint_variance_gap`	Sec. 3.2	$\forall m, a, b, d \in \mathbb{Z},\ d \ne 0 \wedge 4m^2 \le 2a^2 + 2b^2 - d^2 \implies 4m^2 < 2a^2 + 2b^2$.	P,Q
18	`prop23_compression_recurrence_contraction`	Prop. 2.3	$\forall M, J \in \mathbb{N},\ M \ge 2 \implies (M-1)\sum_{r=0}^{J-1} M^r + 1 = M^J$.	P,Q

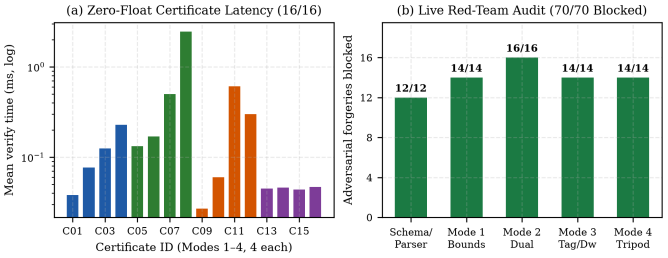

Figure 3: **(a)** Mean exact zero-float verification latency across all 16 canonical certificates (0.027–2.466 ms, log scale). **(b)** Live adversarial red-team audit rejecting 70/70 forgeries across five attack classes with exact error-branch assertions.

4 Exact Findings, Worked Witnesses, and Audit

All experiments ran locally on Windows 11 (Python 3.12.6, Lean 4.35.0; 7-run means after warm-up).

1. Finite-Size Separation, Tripod Rigidity & Exhaustive Tag$(1,1)$ **(Figs. 1–2).** Exact integer-ceiling sweeps across $n \in \{2, 4, \ldots, 4096\}$ show Corollary 1.2's $\lceil n^{9/4} \rceil$ surpassing Landsberg–Michałek's $2n^2 - \lceil \log_2 n \rceil - 1$ by 2.00× at $n = 256$ (262,144 vs. 131,063) and 4.00× at $n = 4096$ (134,217,728 vs. 33,554,419). Figure 2 plots exact rational evaluations of $D^*(1,1,b)$ across $b \in [1/8, 32]$: the ratio Perim$/D^*$ peaks uniquely at 9/4 for $b = 1$ (zero AM–HM defect) and drops to $11/5 = 2.20$ at $(1,2,3)$ (defect 4/33) and $20502/10201 \approx 2.0098$ at $(1,1,100)$ (defect 726/67). Exhaustively enumerating all $2^6 = 64$ inputs to Tag$(1,1)$ confirms 64/64 exact agreement (8 accepted, 56 rejected) with Section 4.1's two-D_w signed-sum reduction.

2. Hand-Verifiable Worked Exact Witnesses (One per Mode).

- **Mode 1 (`C02`, $n = 256 = 2^8$, rect $(16,4,16)$, tight T_6):** $256^9 = 2^{72} = (2^{18})^4$, certifying border rank $\ge 262{,}144 > 2^{17} = 131{,}072$ (refuting Sun [9]) and $\ge 131{,}072$ nonscalar gates; for $T_{16,4,16}$, $(1024)^{3/4} \approx 181.0 < \max(64, 64, 256) = 256$; for T_6 with $B = 7$, all $6^3 = 216$ triples satisfy $(i{-}7j){+}(7j{-}49k){+}(49k{-}i) = 0$ with 36 distinct weights per factor.
- **Mode 2 (`C06`, 2×2 Strassen + division over $\mathbb{F}_{257}[X,Y][u,v]/(u^2, v^2)$):** Routing M_1 through $(M_1 d)/d$ with regular nonconstant $d = a_{00} + b_{11} + 1$ uses 30 gates ($q = 9$ symbolically nonscalar: 8 `mul` + 1 `div`, Lemma 2.4 rank bound $2q = 18$) and symbolically matches $(A_0 + uX)(B_0 + vY)$ across all $1 + 8 + 16 = 25$ coordinates per output entry modulo 257.
- **Mode 3 (`C10`, Tag$(2,2)$, $N = 4$):** On valid permutation $\pi = [2,0,3,1]$ with $x = [1,3,2,0], y = [3,0,1,2]$ ($x_i = y_{\pi(i)}$), $D_w^{(1)} = 1$ and the $2^4 = 16$-term signed sum yields $+1$; mutating $x_3 \to 1$ collapses the signed sum to 0, and colliding $\pi_2 \to 2$ gives $D_w^{(1)} = 0$.
- **Mode 4 (`C13` & `C14`):** On $(1,1,1)$, $D^* = 3 - \frac{1}{3} = \frac{8}{3}$, perimeter = 6, ratio $= 6/(8/3) = 9/4$, AM–HM margin = 0, and $D^*(1,1,5) = 7 - \frac{5}{11} = \frac{72}{11} = 5 + \frac{3}{2} + \frac{1}{22}$. On scale-1 maximal $(\frac{3}{8}, \frac{3}{8}, \frac{3}{8})$ (Cor. 11.1), $D^* = 1$, all three wire lengths equal $\frac{3}{4}$, and perimeter = 9/4.

3. 16-Certificate Atlas & 76-Test Red-Team Audit (Table 2, Fig. 3). Table 2 lists all 16 canonical certificates verified in 0.027–2.466 ms. `tests/test_suite.py` runs 76 pytest checks: 1 full 16-certificate replay, 3 raw-JSON parser guards (float, `NaN`, duplicate keys), 2 exact regressions (exhaustive 64-input Tag$(1,1)$ agreement and balanced tripod peak / Sun $n = 256$ refutation), and 70 parametrized live

Table 2: Canonical 16-certificate `OMEGA94-LB-CERT-1.0` atlas (`exp1_certificate_atlas.json`; all 16 verified).

ID	Certificate Name	M	Exact Certified Witness Summary	ms
C01	`m1_bounds_n16_rect4x4x4`	M1	n=16: $\underline{R} \geq 512$, gates ≥ 256, $T_{4,4,4} \geq 23$	0.038
C02	`m1_bounds_n256_sun_refute`	M1	n=256: $\underline{R} \geq 2^{18} > 2^{17}$, gates ≥ 131072	0.077
C03	`m1_bounds_n1024_rect64x16x64`	M1	n=1024: $\underline{R} \geq 5931642$, T_8 (512 triples)	0.125
C04	`m1_bounds_n4096_rect256x64x256`	M1	n=4096: $\underline{R} \geq 2^{27}$, T_{10} (1000 triples)	0.229
C05	`m2_dual_strassen_2x2_f101`	M2	$\mathbb{F}_{101}$, 2×2 Strassen: q=7, $2q$=14	0.132
C06	`m2_dual_strassen_div_2x2_f257`	M2	$\mathbb{F}_{257}$, 2×2 Strassen+div: q=9, $2q$=18	0.169
C07	`m2_dual_schoolbook_div_3x3_f509`	M2	$\mathbb{F}_{509}$, 3×3 +div: q=29, $2q$=58	0.499
C08	`m2_dual_schoolbook_4x4_f1009`	M2	$\mathbb{F}_{1009}$, 4×4 symbolic: q=64, $2q$=128	2.466
C09	`m3_tag_h1_exhaustive_4cases`	M3	Tag(1, 1) (N=2): 4 instances (2 acc.)	0.027
C10	`m3_tag_h2_valid_and_collisions`	M3	Tag(2, 2) (N=4): 4 instances (16 masks)	0.060
C11	`m3_tag_h3_cyclic_perm_n8`	M3	Tag(3, 3) (N=8): cyclic (256 masks)	0.610
C12	`m3_tag_h3_involution_n8`	M3	Tag(3, 3) (N=8): invol. (256 masks)	0.301
C13	`m4_tripod_balanced_unit_1_1_1`	M4	(1, 1, 1): D^*=8/3, ratio 9/4, margin 0	0.045
C14	`m4_tripod_maximal_scale1_3_8`	M4	$(\frac{3}{8}, \frac{3}{8}, \frac{3}{8})$: D^*=1, wires $\frac{3}{4}$, 9/4	0.046
C15	`m4_tripod_asymmetric_1_2_3`	M4	(1, 2, 3): D^*=60/11, ratio 11/5, marg. 4/33	0.044
C16	`m4_tripod_stretched_1_1_100`	M4	(1, 1, 100): ratio 20502/10201, b=100	0.047

adversarial forgeries (12 schema/parser, 14 Mode 1, 16 Mode 2 including a q=1 single-direction cheat and non-canonical field/constant entries, 14 Mode 3, and 14 Mode 4 including a forged zero-column-sum star matrix), each asserting an exact regex on its intended `CertificateError` branch. `scripts/verify_all.py` enforces all 5 gates including strict axiom whitelisting and a 41-file SHA-256 manifest.

5 Conclusion

We built an independent, explicitly scoped, zero-floating-point verification companion for the discrete algebraic, symbolic dual-number bilinearization, tight-tensor, tagged-permutation, harmonic-star, and tripod AM–HM rigidity mechanisms of OpenAI's $\omega_F = 9/4$ lower-bound preprint [5], pairing 18 constructive Lean 4.35.0 sub-lemmas (zero `sorry`, zero `Classical.choice`) with the pure-`int`/`Fraction` 4-mode auditor `OMEGA94-LB-CERT-1.0`, 16 canonical exact finite witnesses, and 70/70 live adversarial forgery rejections.

References

[1] Alimzhan Amanov, Maxim van den Berg, and Jeroen Zuiddam. Multiplying matrices via polynomials: Exposition and barriers. arXiv:2610.30054v1, 2026.

[2] Markus Bläser. Lower bounds for the bilinear complexity of associative algebras. *Computational Complexity*, 9:73–112, 2000.

[3] Leonardo de Moura and Sebastian Ullrich. The Lean 4 theorem prover and programming language. In *Automated Deduction – CADE 28*, volume 12699 of *LNCS*, pages 625–635. Springer, 2021.

[4] J. M. Landsberg and Mateusz Michałek. A $2n^2 - \log_2(n) - 1$ lower bound for the border rank of matrix multiplication. *International Mathematics Research Notices*, 2018(15):4722–4733, 2018.

[5] OpenAI. The matrix multiplication exponent is nine fourths. Unrefereed Companion Preprint (OpenAI Math Release, https://github.com/openai/math/blob/main/preprints/The-matrix-multiplication-exponent-is-nine-fourths-November-24-2026/paper.pdf), November 2026. Proposes the matching lower bound $\omega_F = 9/4$ over every field, geometric border rank $\geq n^{9/4}$, and $\lceil n^{9/4}/2 \rceil$ nonscalar gates.

[6] OpenAI. An upper bound of 9/4 for the matrix multiplication exponent. OpenAI Math Release Preprint (October 2, 2026; establishes $\omega_{\mathbb{C}} \leq 9/4$), October 2026.

[7] Volker Strassen. Gaussian elimination is not optimal. *Numerische Mathematik*, 13(4):354–356, 1969.

[8] Volker Strassen. Algebra and complexity. In *First European Congress of Mathematics, Vol. II*, volume 120 of *Progress in Mathematics*, pages 429–446. Birkhäuser, 1994.

[9] Zhi-Wei Sun. Tensor degenerations for matrix multiplication. arXiv:2610.13971v1, 2026.